Ghost in the Crystal: Reconstructing the Petrogenic History of Olivine Megacrysts in Martian Basalts Using Phosphorous Zoning. P.M. Aaron, C.K. Shearer, and P.V. Burger. Institute of Meteoritics, Department of Earth and Planetary Sciences, University of New Mexico, Albuquerque, New Mexico 87131.

Introduction: Numerous studies have demonstrated that the distribution of phosphorous in olivine records the kinetic, dynamic, and geochemical state of the magmatic system [1-5]. The formation and preservation of the P zoning contrasts with zoning of divalent cations such as Fe, Mg, and Ca. These differences have been attributed primarily to differences in diffusion [1-5]. Shearer et al. [6] illustrated the chemical differences among olivines from depleted and enriched shergottites, and suggested that parameters such as fO_2 changed more dramatically in the enriched shergottites.

Here, we explore the origin of the olivine megacrysts in Martian olivine-phyric shergottites by combining wavelength-dispersive spectroscopic mapping (WDS) via the Electron Probe Microanalyzer (EPMA), with EPMA spot analyses of olivines from two distinctly different Martian basalts: Northwest Africa 1183 (NWA 1183) and Yamato 980459 (Y 98). It is likely that NWA 1183 represents fragments of NWA 1168/1110 [6]. The key difference between these two samples is that Y 98 is an incompatible element "depleted" shergottite (i.e. depleted LREE pattern, high ε_{Nd}, low I_{Sr}, fO_2 = IW+1), whereas NWA 1183 is an incompatible element "enriched" shergottite (relatively flat REE pattern, low ε_{Nd}, high I_{Sr}, fO_2 ≥IW+2.5).

We reconstructed the early chemical and thermal history in these two distinctly different shergottites by examining P zoning in large olivine megacrysts. We will use this data as a foundation to examine the relationships between intrinsic parameters and geochemical characteristics preserved in these two basalts.

Analytical Approaches: Samples were initially characterized with backscattered electron imaging (BSE) using the JEOL JXA-8200 EPMA in the Department of Earth and Planetary Sciences at the University of New Mexico. Suitable grains were chosen for WDS mapping. Maps were collected for the elements Ti, Cr, P, Ca, Mn, V, Mg, and Fe at a beam current of 500 nA using a spot size of <1 micron, based on the methodology of [7]. WDS maps were used to position traverses for quantitative analysis of the elements Al, Fe, Mg, Si, Ti, Na, Mn, Cr, Ca, P, V, and Ni at a beam current of 20 nA, using a <1 micron spot.

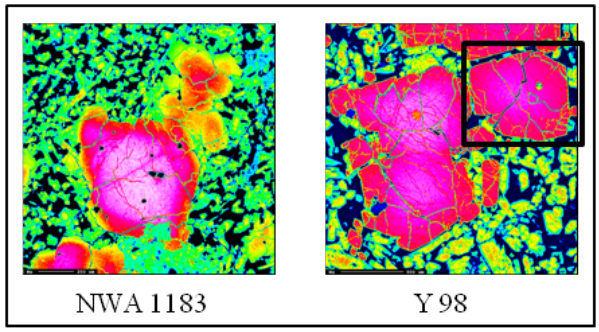

Figure 1. Mg WDS maps of olivine crystals analyzed in this study, showing normal zoning from a high Mg core to a low Mg rim.

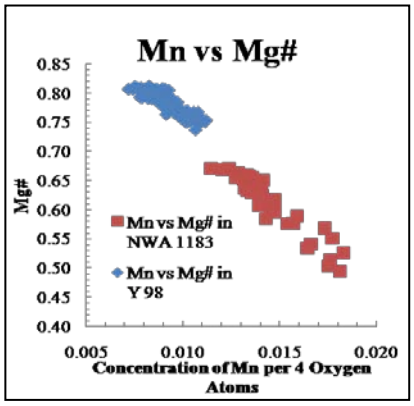

Figure 2. Mn vs. Mg# for NWA 1183 and Y 98 olivine.

Observations: The initial major element maps show that the olivine megacrysts in both NWA 1183 and Y 98 exhibit normal Mg# core to rim zoning with higher Fo content in the core (Fig. 1). The Mg# of the megacrysts in Y 98 is higher than NWA 1183 and there is no overlap in Mg chemistry. Other divalent cations such as Mn, Ca, and Ni generally exhibited a similar zoning style, with Mn and Ca increasing from core to rim and Ni decreasing. Mn is especially correlated to Mg#. The Mn is generally lower in Y 98 compared to NWA 1183 (Fig. 2).

The minor element maps of P reveal a dramatically different zoning style compared to the divalent cations. The P exhibits well-defined oscillatory zoning. The

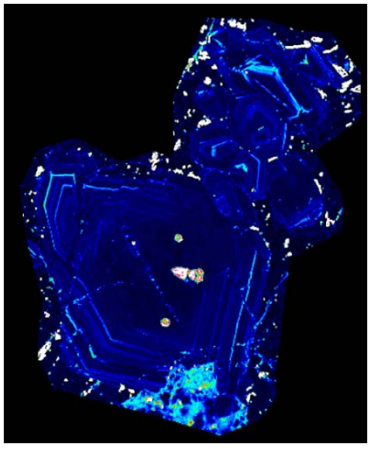

Figure 3. P WDS map of NWA 1183 olivine; Mg map in Fig. 1.

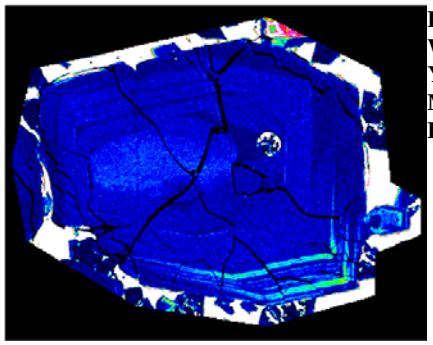

Figure 4. P WDS map of Y 98 olivine; Mg map in Fig. 1.

concentration of P and the P zoning is much more prevalent in NWA 1183 (Fig. 3). There also seems to be a correlation between the location of the zones of P enrichment and proximity to other crystals. For example, in Y 98 the P zoning is far less prominent in the portions of the olivine adjacent to other olivine megacrysts (Figs. 1 and 4). Within the capabilities of the EPMA, there appears to be a slight correlation between P and Al (Fig. 5) and no identifiable correlation between P and either Ti or Cr.

Conclusions: Numerous kinetic factors have been proposed to account for the occurrence of oscillatory P zoning within olivine with well-defined normal growth zoning of divalent cations (Mg, Fe, Mn, Ca, Ni) [1-5]. In the case of these two Martian basalts, we suggest that the formation and preservation of the P concentric zoning is closely tied to the diffusivity of P within both the melt adjacent to the growing olivine megacrysts and the olivine megacrysts themselves. The incompatibility of P in olivine results in higher concentration of P within the melt while slow diffusion leads to the inability to "outrun" the growing olivine crystal faces [2]. Visible P zones are the result of periods of rapid crystal growth due to increases in cooling rate [5]. This mechanism is inhibited in environments in which there are large adjacent megacrysts, as shown in Y 98. This oscillatory zoning is preserved because of the low diffusivity of P in olivine. Aluminum, Cr, and Ti could also exhibit behavior similar to P, however their correlation to P in these basalts is determined by the interplay of several factors such as their respective compatibility in olivine (P<Al<Ti<Cr) [2], diffusivity in both melt and olivine ($D_P<D_{Al}<D_{Ti}<D_{Cr}$) [2], and instrument precision.

Due to the charge (5+) and ionic radius (0.17 Å in 4-fold coordination [8]) of the P cation in magmatic environments, it most readily substitutes into the tetrahedral site of olivine that is occupied predominantly by Si^{4+} (0.26 Å [8]). Phosphorous substitution into this site requires a coupled substitution to maintain charge balance within the crystal structure [2]. The correlation of P and Al in NWA 1183 points to a possible substitution mechanism, initially proposed by [2]:

$$2Si_T^{4+} \leftrightarrow P_T^{5+} + Al_T^{3+}$$

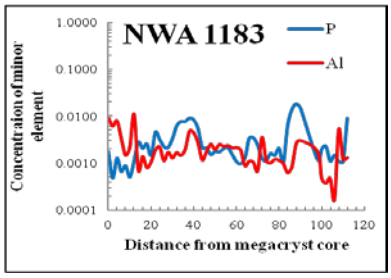

Figure 5. P and Al EPMA traverse in NWA 1183 olivine.

The correlation between Al and P in our data is further complicated by other substitutions into the olivine structure that involve Al, such as:

$$Si_T^{4+} + Mg_O^{2+} \leftrightarrow Al_T^{3+} + Al_O^{3+}$$

The correlation between Al and P can also be further complicated by coupled substitutions that involve P in the tetrahedral site balanced by either vacancies or monovalent cations in the octahedral site (i.e. Li, Na).

Shearer et al [6] illustrated that in many cases the olivine megacrysts in shergottites represent phenocrysts or accumulated phenocrysts and not xenocrysts. This can be important if additional petrogenetic information concerning the shergottites is to be extracted from the individual olivine grains or isotopic systems. Bulk meteorite chemical and isotopic data indicate that Y 98 is a "depleted" shergottite, whereas NWA 1183 is an "enriched" shergottite. Part of this signature is fingerprinted in the P_2O_5 concentration with bulk Y 98 having 0.29% P_2O_5 while enriched shergottites commonly have higher P_2O_5 (currently NWA 1168/1110/1183 have not been analyzed for bulk P_2O_5). The difference in P_2O_5 in the olivine megacrysts in NWA 1183 and Y 98 indicates that the first silicate phase (olivine) crystallized from enriched and depleted basalts, respectively. This suggests that the olivine megacrysts most likely represent phenocrysts and that the enriched and depleted signatures were added to the basalts prior to crystallization. Based on mineral equilibria and vanadium oxybarometry, Herd concluded that the megacrystic olivine in NWA 1168/1110 crystallized at an fO_2 of QFM-2.5, whereas latter phases in the crystallization sequence (including olivine rims) crystallized at an fO_2 of QFM+0.3 [9]. These observations, along with our observations on olivine, indicate that the enriched signature and fO_2 are decoupled and that an enriched and oxidized Martian mantle may not exist.

References: [1] Milman-Baris M. et al. (2008) Contrib. Mineral Petrol 155, 739-765. [2] Spandler and O'Neill (2010) Contrib. Mineral Petrol 159, 791-818. [3] Qian, Q. et al. (2010) Geology 38-4, 331-334. [4] Boesenberg et al. (2004) LPSC XXXV, #1366. [5] Stolper et al. (2009) Eos Trans. AGU, 90(22), Jt. Assem. Suppl., #V74B-01. [6] Shearer et al. (2008) MAPS, 43, 1241-1258. [7] McCanta el al. (2008) LPSC XXXIX, #1807 [8] Shannon and Prewitt (1969) Acta Cryst. 925-946. [9] Herd (2006) Amer. Mineral 91, 1616-1627.